Fluorescent Gold Nanoclusters for Biosensor and Bioimaging Application

Yunlong Bai [1,2], Tong Shu [1,2,3,*], Lei Su [1,2] and Xueji Zhang [1,2,4,*]

[1] Research Center for Biomedical and Health Science, Anhui Science and Technology University, Fengyang 233100, China; b532894237@126.com (Y.B.); sule@ustb.edu.cn (L.S.)

[2] Research Center for Bioengineering and Sensing Technology, School of Chemistry and Biological Engineering, University of Science and Technology Beijing, Beijing 100083, China

[3] Guangdong Provincial Key Laboratory of Luminescence from Molecular Aggregates, South China University of Technology, Guangzhou 510640, China

[4] School of Biomedical Engineering, Shenzhen University Health Science Center, Shenzhen 518060, Guangdong, China

* Correspondence: shutong@ustb.edu.cn (T.S.); zhangxueji@ustb.edu.cn (X.Z.)

Abstract: With the rapid development of materials technology, fluorescent gold nanoclusters (AuNCs) are emerging as novel functional materials for diagnostic applications including the detection of biomarkers and bioimaging due to the advantages of their ultra-small size, tunable emissions, size-dependent fluorescence and excellent biocompatibility. In this review, we introduced the synthetic methods, and physical and chemical properties of AuNCs. Subsequently, we described the AuNCs-based design strategies for the detection of biomarkers including small molecules, DNA and proteins. The applications of AuNCs for tumor imaging in vitro and in vivo were also presented. Finally, we discussed the challenges and potential solutions of AuNCs-based nanosensors.

1. Introduction

A growing number of diseases are seriously endangering human health, and early diagnosis is exceedingly crucial to improve the condition of patients [1–3]. Biomarkers, which are usually found in body fluids including urine or blood, have always been considered as indicators of specific diseases. Rapid, sensitive and cost-effective biosensors for the detection of biomarkers are in high demand, to meet the needs of clinical testing and scientific research [4–6]. The development of special nanomaterials such as fluorescent tags in the last decade is an attractive field due to their potential applications in life sciences [7–10]. Fluorescent nanoclusters (NCs), such as Au, Ag, Pt, Cu, etc., as fluorophores have drawn increasing attention due to their distinctive chemical and physical properties [11–13]. Particularly, fluorescent gold nanoclusters (AuNCs), with their size-dependent chemical, electrical and optical properties, have been widely explored for their fundamental scientific research and diverse biological applications [14–16]. AuNCs are ultra-small particles consisting of several to a few hundred gold atoms. Due to their size approaching the Fermi-wavelength of electrons, between Au atoms and nanoparticles, AuNCs exhibit molecule-like characteristics, such as discrete energy levels, size-dependent fluorescence and strong photoluminescence. Along with the perfect properties of a large Stokes shift, long life-time, good photostability and biocompatibility, AuNCs are suitable candidates for fluorescent probes, for advancing biological applications such as biosensors and molecular imaging [17–19]. Although some reviews have demonstrated the utility of fluorescent AuNCs in sensing and/or imaging, ideas on AuNCs specifically targeting disease-related biomarkers are not well organized.

In this review, we focus on the recent examples of AuNCs that are related to biomarker detection and imaging. Firstly, we update recently reported approaches on the synthesis of fluorescence AuNCs. With the development of methods for preparing varied AuNCs, a series of sensors and probes based on AuNCs have been reviewed regarding diagnostic applications. In addition, we present the sensing strategies, in detail, according to the roles that AuNCs play. Finally, we describe the challenges and possible solutions for the applications of AuNCs in the biosensing and bioimaging field.

2. Synthetic Methods of AuNCs

Both top-down and bottom-up methods are used for the synthesis of AuNCs. In the top-down process, the larger gold nanoparticles are etched by some chemicals (such as thiols, tertiary phosphines) in order to produce ultra-small AuNCs. In the bottom-up approach, the AuNCs are formed by assembling individual Au atoms upon the presence of the precursor [20].

A variety of fluorescent AuNCs with different ligands have been reported using various synthetic approaches. AuNCs are usually formed in the presence of ligands and stabilizing templates, allowing the formation of the ligand shell-Au core structure [21]. The protecting ligands are used to stabilize the AuNCs to avoid aggregation, which plays a vital role in the preparation of AuNCs and influences their fluorescence properties [22]. Biomolecules (DNA, proteins and amino acids) have already been reported as templates or etchants for AuNCs synthesis [23]. The coordination between the biomolecules and the surface of Au have been adopted by maintaining the large steric hindrance and high metal binding affinity, as well as a suitable reducing ability without needing other reducing agents [24]. The synthesis of AuNCs using diverse templates were introduced as following:

2.1. AuNCs Synthesized Using Proteins as the Templates

The most commonly used approach for the fabrication of AuNCs are protein template syntheses. Bovine serum albumin (BSA) is firstly used as the template to synthesize AuNCs [25]. Following that, a range of other proteins, including human serum protein, ovalbumin, transferrin protein lysozymes, insulin, etc., have been used as templates for the synthesis of AuNCs [21].

2.2. AuNCs Synthesized Using Peptides as the Templates

The surface functional properties and size of AuNCs play critical roles in sensing and bioimaging applications, and AuNCs synthesized using peptides as templates can achieve such goals. The composition of amino acids in peptides greatly influences the physical and chemical properties of the AuNCs [26]. For example, cysteine (Cys) with thiol groups plays a key role in reducing and chelating metal ions during the formation of AuNCs. Glutathione (Glu-Cys-Gly, GSH), as a classical thiolate ligand has also been successfully used to prepare AuNCs, through the strong binding of Cys residues and AuNCs. Additionally, targeting imaging of diverse cancer-specific proteins by changing the amino acid composition in the functional region was successfully achieved [24].

2.3. AuNCs Synthesized Using DNA as the Template

DNA has usually been considered as the template for the synthesis of fluorescent AuNCs, which has several advantages as follows: Firstly, unlike some synthetic chemicals, non-toxic DNA has great biocompatibility. Secondly, many functional DNA can perform the molecular recognition roles. The appropriate design of DNA sequences enables direct analyte binding and fluorescence signal reading. Thirdly, chemical synthesized DNA can easily be modified with functional groups, which can facilitate the applications of DNA-templated AuNCs [27,28].

3. Applications of AuNCs-Based Biosensors

An efficient fluorescent sensor incorporates both recognition components, to provide selective interaction, and the analytes and transducer parts to signal the interaction through signal changes.

AuNCs, with properties such as a large Stokes shift, long lifetime and excellent biocompatibility, can specifically interact with target analytes as the recognition components or fluorescence tag, in an AuNCs-based fluorescent sensing platform. Compared with other fluorescent analysis methods, AuNCs-based fluorescent sensors have some advantages, such as being easy to synthesize, high sensitivity, and having a high fluorescence quantum yield. In addition, AuNCs are easy to conjugate with functional molecules such as recognition molecules, fluorescent dyes, drugs, etc., to enlarge the application scope of AuNCs. A variety of AuNCs-based fluorescent sensors have been developed for the detection of biomolecules such as DNA, microRNA, small molecules and proteins, which are described in detail in the following sections. Table 1 shows the AuNCs-based biosensors for the detection of diverse targets by comparison of design strategy, fluorescence signal, response type, detection limit and dynamic range.

Table 1. AuNCs-based fluorescence biosensors for detection of diverse targets.

Target	Design Strategy	Fluorescence Signal	Response Type	Detection Limit	Dynamic Range	Ref
microRNA-21	DNA-AuNCs	Single	on	0.7 pM	1 pM–10 nM	[29]
DNA Thrombin	DNA-AuNCs-MnO$_2$	Single	on	0.2 nM 0.1 nM	0.5–20 nM 0.2–20 nM	[30]
Glucose	Ovalbumin-AuNCs	Ratiometric	on	0.1 mM	0.50–10.0 mM	[31]
5-HT	Transferrin-AuNCs	Single	on	0.049 μM	0.2–50 μM	[32]
Cys Hcy	BSA-AuNCs	Single	on	9 nM 12 nM	0.0057–5 μM 8–25 μM	[33]
Cys	BSA- AuNCs	Single	on	1.2 nM	2–800 nM	[34]
Cys	BSA- AuNCs	Single	off	6.3 pM	10 pM–2 mM	[35]
Cys	BSA-AuNCs	Single	off	0.15 μM	0.5–10 μM	[36]
TCEP	BSA-AuNCs	Ratiometric	on	0.13 μM	0.5–50 μM	[37]
GSH	BSA-AuNCs	Single	on	0.1 mM	0.1–2.0 mM	[38]
H$_2$S	BSA-AuNCs-FITC	Ratiometric	on	0.73 μM	7–100 μM	[39]
HDAC 1 PKA	Peptide-AuNCs	Single	off	5 pM 6 pM	15 pM–30 nM 15 pM–60 nM	[40]
MMP-9	Peptide-AuNCs-GO	Single	on	2.5 ng/mL	5–20 ng/mL	[41]
PKA	Peptide-AuNCs	Single	on	0.02 U/mL	0.05–1.6 U/mL	[42]
PKA	Peptide-AuNCs	Single	on	0.004 U/L	0.01–40 UmL	[43]
Trypsin	Glutathione-AuNCs	Single	on	0.08 μg/mL	0.2–100 μg/mL	[44]
GSH GR	Cytidine-AuNCs	Single	on	2.0 nM 0.34 U/L	20 nM–3 μM 0.34–17.0 U/L	[45]
ALP	BSA-AuNCs	Single	on	0.16 U/mL	1–6 U/mL	[46]
ALP	GSH-AuNCs-SiNPs	Ratiometric	on	0.23U/L	0.5–10 U/L	[47]
Heparin Trypsin ALP	Peptide-AuNCs	Single	off off on	3 nM 0.3 nM 0.3 U/L	8–80 nM 1–100 nM 1–10 U/L	[48]
Epinephrine	BSA-AuNCs	Single	off	587 pM	10–100 μM	[49]
kynurenine	γ-globulin-AuNCs	Single	off	5 μM	15–100 μM	[50]
Tyrosinase Dopamine	GSH-AuNCs	Ratiometric	on	0.006 U/mL 1 nM	0.006–3.6 U/mL 1 nM–1 mM	[51]

5-HT, 5-hydroxytryptamine; Cys, cysteine; Hcy, homocysteine; BSA, bovine serum albumin; PKA, protein kinase A; ALP, alkaline phosphatase; Glutathione reductase, GR; ALP, Alkaline phosphatase; GO, graphene oxide; MMP-9, Matrix metalloproteinase-9; Glutathione, GSH; HDAC 1, histone deacetylase 1; SiNPs, silicon nanoparticles; NBD, 7-nitro-2,1,3-benzoxadiazole; TCEP, tris (2-carboxyethyl) phosphine; H$_2$S, hydrogen sulfide; FITC, fluorophore; SiNPs, silicon nanoparticles.

3.1. AuNCs-Based Fluorescent Sensors for Detection of DNA and MicroRNA

Hosseini et al. showed a fluorescence turn-on biosensor for the detection of microRNA [29]. AuNCs were synthesized by templated DNA, containing the complementary sequence of target

microRNA and two cytosine rich sequence fragments at the 3′ and 5′ ends. The addition of microRNA-21 led to an increased fluorescence intensity. This sensor had a detection limit of 0.7 pM. Wang et al. reported a fluorescent biosensing platform for DNA detection through the combination of DNA-templated AuNCs (DNA-AuNCs) and MnO_2 sheets [30]. This strategy was based on the specific binding of DNA-AuNCs probe towards targets and the different adsorption between DNA structures and MnO_2. The detection limit of this assay was 0.2 nM DNA. Similarly, when using aptamer as affinity ligands, an AuNCs-based fluorescent sensor could be used for thrombin detection.

3.2. AuNCs-Based Fluorescent Sensors for Detection of Small Molecules with Biological Activity

AuNCs-based biosensors for the detection of small biological molecules had been achieved using various design strategies. Mao reported a ratiometric fluorescent probe for sensing glucose, one of the most significant biomolecules in the biological systems [31]. Ovalbumin protected AuNCs (Ova-AuNCs), with good emission and perfect biocompatibility was used as fluorescent tag. Poly(N-acryloxysuccinimide)-aminophenyl boronic acid-Alizarin Red S (PNAS-APBA-ARS) was used as the response signal probe and specific recognition element for the detection of the target. The detection of this biosensor was 0.1 mM glucose. Sha et al. reported a fluorescence biosensor for the sensitive detection of 5-hydroxytryptamine (5-HT), using transferrin-encapsulated AuNCs [32]. As shown in Figure 1, the presence of 5-HT induced an aggregation-enhanced emission of transferrin-AuNCs due to the high affinity between sialic acid residues of transferrin and 5-HT. The changing of the fluorescence signal was used for the quantitative detection of 5-HT, in the range from 0.2 to 50 μM with a detection limit of 0.049 μM. Zhang et al. presented histidine-templated AuNCs for the fluorescence sensing of Glutathione (GSH). The addition of GSH could induce an enhancement of the fluorescence intensity of AuNCs, enabling the quantitative detection of the target with a detection limit of 25 μM [52]. Vitamins, associated with many metabolic processes of sugars and proteins, play a vital role in human health. Liu et al. displayed a fluorescence sensor for the quantitative detection of Vitamin B_1, using glutenin-templated AuNCs [53]. Target vitamin could be adsorbed on the surface of glutenin-AuNCs with numerous hydroxyl and carboxyl groups, and fluorescence-quenching signals were measured for sensing targets with a detection limit of 115 nM. BSA-stabilized AuNCs were used for sensing cysteine (Cys) and homocysteine (Hcy) [33]. In this approach, the fluorescence of BSA-AuNCs was quenched by potassium triiodide. In the presence of target Cys and Hcy, the fluorescence recovered through the removement of iodine. The turn-on response enabled the sensitive detection of target molecules. Cui et al. used the BSA-AuNCs-based nanoplatform for the detection of Cys [34]. After the addition of Cys, the forming of Cys-AuNCs complexes enhanced the fluorescence signal, allowing for the quantitative detection of Cys, with a detection limit of 1.2 nM.

Our group reported pH-sensitive AuNCs protected by GSH, for the sensitive detection of Cys by chemical etching [35]. AuNCs, presented in an acidic solution with excess Au(I)-thiolate complexes, showed a pH-sensitive permeability for target Cys, which affected the access of Cys to the embedded AuNCs. Cys enhanced the emission of AuNCs; however, Cys at higher concentrations etched the AuNCs, which induced fluorescence quenching, showing an increased pH signal. This sensor exhibited an ultra-wide linear concentration range from 10 pM to 2 mM and an ultra-low detection limit of 6.3 pM. In addition, we described a novel BSA-AuNCs based fluorescent sensor for the label-free, separation-free and selective detection of Cys [36]. The presence of target Cys could cause etching-induced fluorescence quenching of BSA-AuNCs, allowing the sensitive detection of Cys in the range from 0.5 to 10 μM. The detection limit for Cys was 0.15 μM. Our group also presented a chemical etching of an AuNCs-based ratiometric fluorescent sensor for the sensitive detection of tris(2-carboxyethyl)phosphine (TCEP) [37]. The fluorescence spectrum indicated that TCEP could quench the red fluorescent emission of BSA-AuNCs and restore the blue fluorescent emission. The ratio of the blue and red fluorescence intensity of BSA-AuNCs allowed for the quantitative detection of TCEP, with a detection limit of 130 nM.
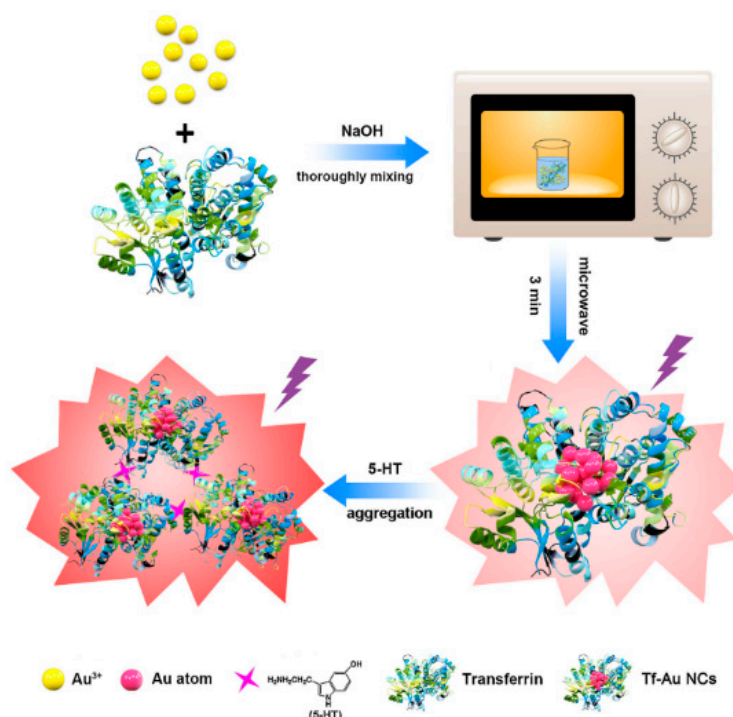
Figure 1. Diagram of the synthesis and detection application of transferrin-AuNCs for fluorescent detection of 5-HT. Reprinted with permission [32]. Copyright 2019 Elsevier B.V.

Lin et al. demonstrated an AuNCs-based turn-on sensor for GSH detection [38]. The fluorescence of BSA-AuNCs was quenched by MnO_2, and in the presence of GSH, MnO_2 was digested and the recovered fluorescence was measured to determine the GSH concentration. Yan et al. presented a ratiometric biosensor for the detection of hydrogen sulfide (H_2S) [39]. BSA-templated AuNCs were used as the internal reference fluorescent tag and HSip-1 acted as the recognition element and signal indicator. The addition of target H_2S enhanced the fluorescence of HSip-1 without affecting the change in BSA-AuNCs fluorescence. Subsequently, the change of ratiometric signal enabled the sensing of the target molecular, with a detection limit of 0.73 μM.

3.3. AuNCs-Based Biosensor for Detection of Proteins

Nguyen et al. presented a turn-on fluorescent AuNCs-graphene oxide (GO) nanosensor for the detection of matrix metalloproteinase-9 (MMP-9) [41]. As illustrated in Figure 2, the AuNCs were synthesized by using peptides and mercaptoundecanoic acid (MUA) as co-templating ligands. The peptide contained an MMP-9 cleavage site. The AuNCs were then loaded to GO, with excellent quenching properties. In the presence of the target enzyme, peptide-AuNCs-GO nanocomplex yielded an increasing fluorescent signal related to the enzyme MMP-9 concentration. The detection limit of this biosensor was 2.5 ng/mL. Liu et al. reported an AuNCs-based fluorescent sensor for the label-free and sensitive detection of protein kinase (PKA) [42]. This approach was based on the Eu^{3+}-modulated fluorescence of peptide-templated AuNCs and the PKA-catalyzed hydrolysis. This turn-on method showed a detection limit of 0.02 U/mL PKA. Song developed a peptide-AuNCs-based fluorescence sensor for monitoring PKA detection [43]. The fluorescence quenching of AuNCs occurred due to the cleavage of peptide by carboxypeptidase, without peptide phosphorylation. The adding of PKA induced the phosphorylation of peptide, therefore, the phosphate group could block the digestion of carboxypeptidase, which prevented the fluorescence quenching of the peptide-AuNCs. The measurement of fluorescence intensity change allowed for the detection of PKA.
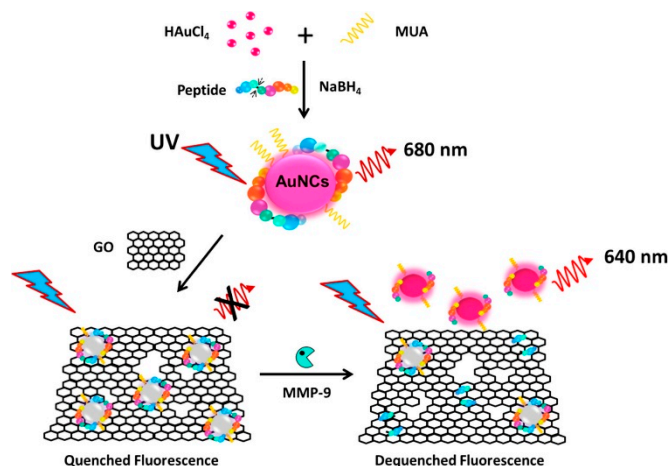
Figure 2. Diagram of peptide-AuNCs-GO nanocomplex for the detection of MMP-9 enzyme. Reprinted with permission [41], Copyright 2015 Elsevier B.V.

GSH-stabilized AuNCs were used for the fluorescence detection of trypsin [44]. The fluorescence of GSH-AuNCs could be quenched by the addition of cytochrome c, through the electron transfer mechanism. The presence of trypsin induced the hydrolysis of cytochrome c. Thereby, a significant fluorescence recovery was observed, and the enhanced fluorescence signal enabled the detection of trypsin, with a detection limit of 0.08 µg/mL and a dynamic detection range from 0.2 to 100 µg/mL. As shown in Figure 3, these GSH-AuNCs could be integrated into portable test strips, which show promising potential for point-of-care detection.
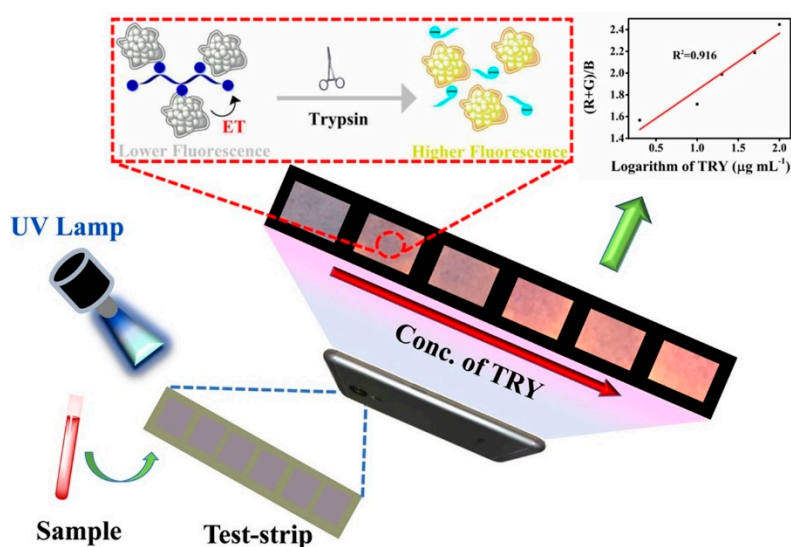
Figure 3. Schematic diagram of the fluorescence sensor for the detection of target trypsin using GSH-stabilized AuNCs. Reprinted with permission [44], Copyright 2018 Elsevier B.V.

The fluorescence enhancement was usually triggered by bio-thiols, due to the AuNCs etch by thiols. Jiang et al. reported a cytidine stabilized AuNCs (Cyt-AuNCs) for sensing GSH, the enhancement of fluorescence intensity enabled the quantitative detection of targets, with a detection limit of 2.0 nM. This platform also allowed for the determination of glutathione reductase (GR) activity, through controlling the production of GSH [45]. Ni et al. showed an AuNCs-based dual-channel assay for turn-on fluorescent and colorimetric sensing of alkaline phosphatase (ALP) [46]. Colorless 3,3′,5,5′-tetramethylbenzidine (TMB) was oxidized into blue product (oxTMB) by BSA- AuNCs with peroxidase-like activity. The production of oxTMB induced the quenching effect of the AuNCs. The addition of ALP, with the ability to catalyze the hydrolysis of L-ascorbic acid-2-phosphate, produced ascorbic acid, which inhibited

the oxidation of TMB. A fluorescence recovery signal was observed. This dual-readout sensor for ALP activity detection was 0.26 and 0.16 mU/mL by colorimetric and fluorescent methods, respectively. Qu et al. reported a ratiometric fluorescent assay for ALP detection, based on the combination of the GSH-AuNCs and SiNPs [47]. The aggregation-induced emission of AuNCs was quenched by $KMnO_4$ and the addition of ALP generated ascorbic acid could reduce $KMnO_4$ to Mn^{2+}. The ratiometric fluorescence of AuNCs and SiNPs enabled the detection of ALP.

3.4. AuNCs for In Vivo Tumor Imaging

AuNCs were good candidates for the agents of metabolism studies in cells and tumor imaging in vivo, due to their distinctive properties: good stability, large Stokes shift, easy modification, good biocompatibility, low intrinsic toxicity, etc. [24]. AuNCs had the capability to combine diverse biomolecules on one system and simultaneously achieve high resolution and sensitivity, which could give more detailed anatomical or biological information [17].

Lu et al. presented a fluorescent dual-emission sensor for living cell imaging, as displayed in Figure 4 [54]. GSH-templated AuNCs (GSH-AuNCs) with oligoarginine linker peptide were decorated with silica particles via streptavidin-biotin interaction. The fluorescence intensity of GSH-AuNCs could be sensitively and selectively quenched by highly reactive oxygen species (hROS), enabling the bioimaging in live cells. Gao et al. demonstrated a facile one-pot strategy for synthesizing fluorescent AuNCs, by using 2-mercapto-5-benzimidazolesulfonic acid (MBISA) as both a protecting and reducing reagent [55]. The MBISA-AuNCs had been applied in hydrogen sulfide detection, cell imaging and pH sensing, which showed multifunctional application in life sciences.
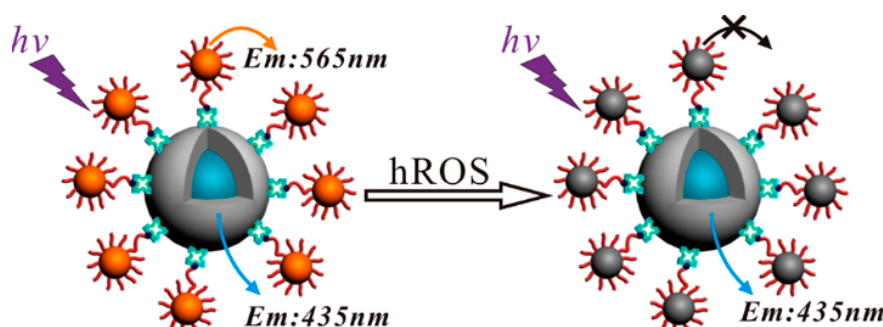

Figure 4. A fluorescent nanoplatform of AuNCs decorated silica particles for live cell imaging. Reprinted with permission [54]. Copyright 2013 American Chemical Society.

Attaching multiple types of ligands (small molecules, peptides, oligonucleotides, antibodies, etc.) to the AuNCs surface facilitates the achievement of tumor targeting. For instance, folic acid is commonly used for recognizing folate receptors, which are over-expressed in diverse tumor cells. Ding et al. demonstrated an AuNCs-based fluorescence biosensor for targeted imaging in cancer cells [56]. As shown in Figure 5, the combination of fluorescein and folic acid on BSA-AuNCs enabled the pH determination and targeted imaging of folate acceptor-rich cancer cells simultaneously.

Hyaluronic acid (HA), a well-known marker for cancer cells, can bind with the receptor CD44 in the membrane of the tumor cell. Zhang et al. reported BSA-AuNCs for tumor-targeted imaging in vivo [57]. The uptake of AuNCs by both cancer cells and tumor-bearing mice can be improved by the modification of FA and HA. Chen et al. presented a near-infrared fluorescent dye conjugated BSA-AuNCs for tumor imaging. The decoration of FA increased the tumor targeting capability of AuNCs [58]. Similarly, Pyo et al. synthesized FA-functionalized GSH-stabilized AuNCs for bioimaging [59].
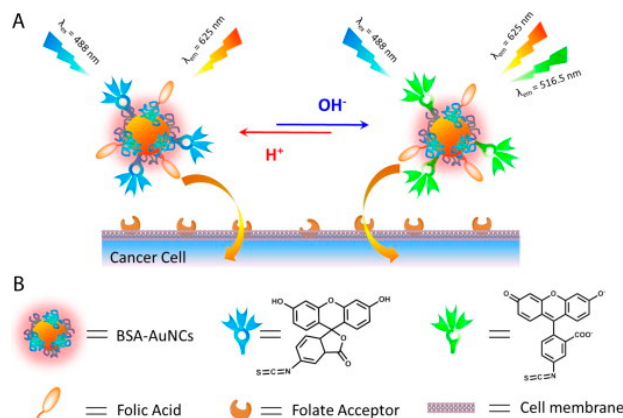
Figure 5. (**A**) Principle of folic acid and fluorescein functionalized AuNCs fluorescent biosensor for cancer cell-targeted imaging and pH detection, (**B**) Structure of AuNCs and decorated ligands. Reprinted with permission [56]. Copyright 2014, Elsevier B.V.

Another common ligand is cyclic RGD (cRGD), which has the ability to bind $\alpha_v\beta_3$ integrins, over-expressed on the surface of tumor cells. Additionally, aptamer AS1411 has a high affinity against nucleolin, over-expressed in the nucleus and cytoplasm of tumor cells. Dual targeting fluorescent AuNCs for bio-imaging and tissue therapy were presented by Chen et al [60]. As shown in Figure 6, cRGD and aptamer AS1411 were used to recognize proteins in the surface of tumor cell and in the nucleus inside of tumor cells, respectively, which greatly enhanced the specificity to tumors. In addition, AuNCs-cRGD-Aptamer was decorated with near infrared fluorescence dye and doxorubicin, giving a fluorescent dual-targeting probe for tumor imaging and tissue therapy. This nanoplatform displayed low cytotoxicity and tumor-targeting capability at both the in vitro and in vivo levels. This assay showed potential for clinical application in tumor imaging.
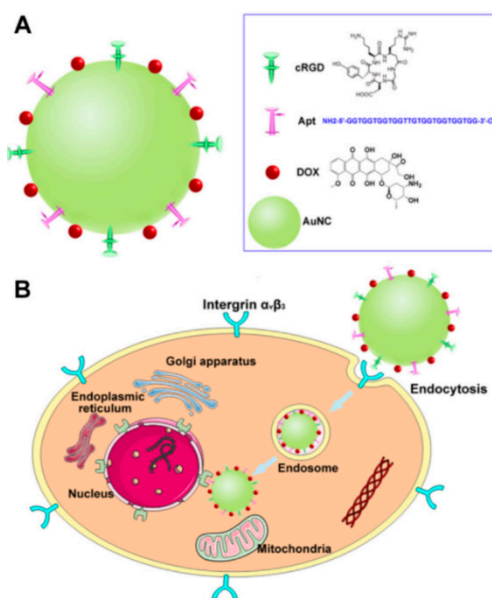

Figure 6. (**A**) Diagram of functionalized AuNCs, (**B**) Schematic illustration of dual targeting AuNCs for tumor imaging and therapy. Reprinted with permission [60], Copyright 2016 Elsevier Ltd.

Li reported a water-soluble eptifibatide stabilized AuNCs fluorescence probe for in vitro cancer cell imaging [61]. The cell imaging experiments demonstrated that eptifibatide-AuNCs could stain the cell membrane and cytoplasm of tested cancer cells, which enabled the applications of this AuNCs-based fluorescence probe in biological analysis. The facile synthesis of L-carnosine-templated fluorescent

AuNCs for cellular imaging was indicated [62]. The L-carnosine-AuNCs exhibited fluorescence emission signals, which could be applied as a fluorescent probe for HeLa cell imaging with good stability and low cytotoxicity. Pea protein isolate (PPI) was used as a stabilizing and reducing agent to fabricate PPI-AuNCs, which showed great capability as a bioimaging probe in cell imaging [63]. Cell membrane coated PPI-AuNCs greatly enhance the tumor enrichment ability and blood circulation properties.

4. Conclusions and Outlooks

This review summarizes the development of fluorescent AuNCs and their applications for biosensing and bioimaging. The large Stokes shift, high fluorescence, tunable emissions, excellent stability and good biocompatibility give fluorescent AuNCs huge potential for diagnostic applications including analytical tests and bioimaging. Although significant progress has already been achieved in recent decades, challenges still exist and great efforts still need to be taken. Firstly, some AuNCs have low fluorescence quantum yields, which significantly affects the detection limits of analyte. Secondly, the structures of AuNCs remain unclear in many cases, and new methods should be established to identify the structure of AuNCs. Thirdly, for bio-imaging in vivo, the metabolic kinetics of AuNCs and toxicity must be further explored. Currently, these fluorescent AuNCs have already shown their potential as promising luminescent probe for biosensing and bioimaging; however, there are still several issues that need to be resolved.

Conflicts of Interest: The authors declare no conflict of interest.

References

1.　Ye, F.; Zhao, Y.; Ei-Sayed, R.; Muhammed, M.; Hassan, M. Advances in nanotechnology for cancer biomarkers. *Nano Today* **2018**, *18*, 103–123. [CrossRef]

2.　Perfezou, M.; Turner, A.; Merkoci, A. Cancer detection using nanoparticle-based sensors. *Chem. Soc. Rev.* **2012**, *41*, 2606–2622. [CrossRef]

3.　Vaidyanathan, R.; Soon, R.H.; Zhang, P.; Jiang, K.; Lim, C.T. Cancer diagnosis: From tumor to liquid biopsy and beyond. *Lab Chip* **2019**, *19*, 11–34. [CrossRef] [PubMed]

4.　De La Franier, B.; Thompson, M. Early stage detection and screening of ovarian cancer: A research opportunity and significant challenge for biosensor technology. *Biosens. Bioelectron.* **2019**, *135*, 71–81. [CrossRef] [PubMed]

5.　Xu, T.; Xu, L.-P.; Zhang, X.; Wang, S. Bioinspired superwettable micropatterns for biosensing. *Chem. Soc. Rev.* **2019**, *48*, 3153–3165. [CrossRef] [PubMed]

6.　Jayanthi, V.S.P.K.S.A.; das, A.B.; Saxena, U. Recent advances in biosensor development for the detection of cancer biomarkers. *Biosens. Bioelectron.* **2017**, *91*, 15–23. [CrossRef]

7.　Yao, J.; Yang, M.; Duan, Y. Chemistry, biology, and medicine of fluorescent nanomaterials and related systems: New insights into biosensing, bioimaging, genomics, diagnostics, and therapy. *Chem. Rev.* **2014**, *114*, 6130–6178. [CrossRef]

8.　Wong, X.Y.; Sena-Torralba, A.; Alvarez-Diduk, R.; Muthoosamy, K.; Merkoci, A. Nanomaterials for nanotheranostics: Tuning their properties according to disease needs. *ACS Nano* **2020**, *14*, 2585–2627. [CrossRef]

9.　Menon, J.U.; Jadeja, P.; Tambe, P.; Vu, K.; Yuan, B.; Nguyen, K.T. Nanomaterials for Photo-Based Diagnostic and Therapeutic Applications. *Theranostics* **2013**, *3*, 152–166. [CrossRef]

10.　Smith, B.R.; Gambhir, S.S. Nanomaterials for in vivo imaging. *Chem. Rev.* **2017**, *117*, 901–986. [CrossRef]

11.　Zhang, L.; Wang, E. Metal nanoclusters: New fluorescent probes for sensors and bioimaging. *Nano Today* **2014**, *9*, 132–157. [CrossRef]

12. Tao, Y.; Li, M.; Ren, J.; Qu, X. Metal nanoclusters: Novel probes for diagnostic and therapeutic applications. *Chem. Soc. Rev.* **2015**, *44*, 8636–8663. [CrossRef] [PubMed]

13. Shang, L.; Dong, S.; Nienhaus, G.U. Ultra-small fluorescent metal nanoclusters: Synthesis and biological applications. *Nano Today* **2011**, *6*, 401–418. [CrossRef]

14. Shu, T.; Wang, J.; Su, L.; Zhang, X. Luminescent Organometallic Nanomaterials with Aggregation-Induced Emission. *Crit. Rev. Anal. Chem.* **2018**, *48*, 330–336. [CrossRef] [PubMed]

15. Zhang, E.; Xiang, S.; Fu, A. Recent progresses of fluorescent gold nanoclusters in biomedical applications. *J. Nanosci. Nanotechnol.* **2016**, *16*, 6597–6610. [CrossRef]

16. Nie, L.; Xiao, X.; Yang, H. Preparation and biomedical applications of gold nanocluster. *J. Nanosci. Nanotechnol.* **2016**, *16*, 8164–8175. [CrossRef]

17. Li, H.; Li, H.; Wan, A. Luminescent gold nanoclusters for in vivo tumor imaging. *Analyst* **2020**, *145*, 348–363. [CrossRef]

18. Maity, S.; Bain, D.; Patra, A. An overview on the current understanding of the photophysical properties of metal nanoclusters and their potential applications. *Nanoscale* **2019**, *11*, 22685–22723. [CrossRef]

19. Cui, M.; Zhao, Y.; Song, Q. Synthesis, optical properties and applications of ultra-small luminescent gold nanoclusters. *TrAC Trends Anal. Chem.* **2014**, *57*, 73–82. [CrossRef]

20. Ungor, D.; Dekany, I.; Csapo, E. Reduction of tetrachloroaurate(III) ions with bioligands: Role of the thiol and amine functional groups on the structure and optical features of gold nanohybrid systems. *Nanomaterials* **2019**, *9*, 1229. [CrossRef]

21. Sun, J.; Jin, Y. Fluorescent Au nanoclusters: Recent progress and sensing applications. *J. Mater. Chem. C* **2014**, *2*, 8000–8011. [CrossRef]

22. He, Z.; Shu, T.; Su, L.; Zhang, X. Strategies of luminescent gold nanoclusters for chemo-/bio-sensing. *Molecules* **2019**, *24*, 3045. [CrossRef] [PubMed]

23. Wang, J.X.; Goswami, N.; Shu, T.; Su, L.; Zhang, X.J. pH-Responsive aggregation-induced emission of Au nanoclusters and crystallization of the Au(I)-thiolate shell. *Mater. Chem. Front.* **2018**, *2*, 923–928. [CrossRef]

24. Zhang, Y.; Zhang, C.Y.; Xu, C.; Wang, X.L.; Liu, C.; Waterhouse, G.I.N.; Wang, Y.L.; Yin, H.Z. Ultrasmall Au nanoclusters for biomedical and biosensing applications: A mini-review. *Talanta* **2019**, *200*, 432–442. [CrossRef] [PubMed]

25. Xie, J.P.; Zheng, Y.G.; Ying, J.Y. Protein-Directed Synthesis of Highly Fluorescent Gold Nanoclusters. *J. Am. Chem. Soc.* **2009**, *131*, 888–889. [CrossRef]

26. Wang, B.; Zhao, M.; Mehdi, M.; Wang, G.; Gao, P.; Zhang, K.-Q. Biomolecule-assisted synthesis and functionality of metal nanoclusters for biological sensing: A review. *Mater. Chem. Front.* **2019**, *3*, 1722–1735. [CrossRef]

27. Kennedy, T.A.C.; MacLean, J.L.; Liu, J. Blue emitting gold nanoclusters templated by poly-cytosine DNA at low pH and poly-adenine DNA at neutral pH. *Chem. Commun.* **2012**, *48*, 6845–6847. [CrossRef]

28. Liu, J. DNA-stabilized, fluorescent, metal nanoclusters for biosensor development. *TrAC Trends Anal. Chem.* **2014**, *58*, 99–111. [CrossRef]

29. Hosseini, M.; Ahmadi, E.; Borghei, Y.-S.; Reza Ganjali, M. A new fluorescence turn-on nanobiosensor for the detection of micro-RNA-21 based on a DNA–gold nanocluster. *Methods Appl. Fluores.* **2017**, *5*, 015005. [CrossRef]

30. Wang, H.-B.; Li, Y.; Bai, H.-Y.; Liu, Y.-M. DNA-templated Au nanoclusters and MnO_2 sheets: A label-free and universal fluorescence biosensing platform. *Sens. Actuators B Chem.* **2018**, *259*, 204–210. [CrossRef]

31. Wang, L.L.; Qiao, J.; Liu, H.H.; Hao, J.; Qi, L.; Zhou, X.P.; Li, D.; Nie, Z.X.; Mao, L.Q. Ratiometric fluorescent probe based on gold nanoclusters and alizarin red-boronic acid for monitoring glucose in brain microdialysate. *Anal. Chem.* **2014**, *86*, 9758–9764. [CrossRef]

32. Sha, Q.; Sun, B.; Yi, C.; Guan, R.; Fei, J.; Hu, Z.; Liu, B.; Liu, X. A fluorescence turn-on biosensor based on transferrin encapsulated gold nanoclusters for 5-hydroxytryptamine detection. *Sens. Actuators B Chem.* **2019**, *294*, 177–184. [CrossRef]

33. Nebu, J.; Anjali Devi, J.S.; Aparna, R.S.; Aswathy, B.; Lekha, G.M.; Sony, G. Potassium triiodide-quenched gold nanocluster as a fluorescent turn-on probe for sensing cysteine/homocysteine in human serum. *Anal. Bioanal. Chem.* **2019**, *411*, 997–1007. [CrossRef] [PubMed]

34. Cui, M.L.; Liu, J.M.; Wang, X.X.; Lin, L.P.; Jiao, L.; Zhang, L.H.; Zheng, Z.Y.; Lin, S.Q. Selective determination of cysteine using BSA-stabilized gold nanoclusters with red emission. *Analyst* **2012**, *137*, 5346–5351. [CrossRef] [PubMed]

35. Wang, J.; Lin, X.; Su, L.; Yin, J.; Shu, T.; Zhang, X. Chemical etching of pH-sensitive aggregationinduced emission- active gold nanoclusters for ultra- sensitive detection of cysteine. *Nanoscale* **2019**, *11*, 294–300. [CrossRef] [PubMed]

36. Shu, T.; Su, L.; Wang, J.; Li, C.; Zhang, X. Chemical etching of bovine serum albumin-protected Au-25 nanoclusters for label-free and separation-free detection of cysteamine. *Biosens. Bioelectron.* **2015**, *66*, 155–161. [CrossRef]

37. Shu, T.; Wang, J.; Su, L.; Zhang, X. Chemical Etching of Bovine Serum Albumin-Protected Au25 Nanoclusters for Label-Free and Separation-Free Ratiometric Fluorescent Detection of Tris(2-carboxyethyl)phosphine. *Anal. Chem.* **2016**, *88*, 11193–11198. [CrossRef]

38. Lin, S.; Cheng, H.; Ouyang, Q.; Wei, H. Deciphering the quenching mechanism of 2D MnO_2 nanosheets towards Au nanocluster fluorescence to design effective glutathione biosensors. *Anal. Meth.* **2016**, *8*, 3935–3940. [CrossRef]

39. Yang, Y.; Lei, Y.; Zhang, X.; Zhang, S. A ratiometric strategy to detect hydrogen sulfide with a gold nanoclusters based fluorescent probe. *Talanta* **2016**, *154*, 190–196. [CrossRef]

40. Wen, Q.; Gu, Y.; Tang, L.-J.; Yu, R.-Q.; Jiang, J.-H. Peptide-Templated Gold Nanocluster Beacon as a Sensitive, Label-Free Sensor for Protein Post-translational Modification Enzymes. *Anal. Chem.* **2013**, *85*, 11681–11685. [CrossRef]

41. Nguyen, P.D.; Cong, V.T.; Baek, C.; Min, J. Fabrication of peptide stabilized fluorescent gold nanocluster/ graphene oxide nanocomplex and its application in turn-on detection of metalloproteinase-9. *Biosens. Bioelectron.* **2017**, *89*, 666–672. [CrossRef]

42. Liu, Q.; Na, W.; Wang, L.; Su, X. Gold nanocluster-based fluorescent assay for label-free detection of protein kinase and its inhibitors. *Microchim. Acta* **2017**, *184*, 3381–3387. [CrossRef]

43. Song, W.; Liang, R.-P.; Wang, Y.; Zhang, L.; Qiu, J.-D. Green synthesis of peptide-templated gold nanoclusters as novel fluorescence probes for detecting protein kinase activity. *Chem. Commun.* **2015**, *51*, 10006–10009. [CrossRef]

44. Li, H.; Yang, M.; Kong, D.; Jin, R.; Zhao, X.; Liu, F.; Yan, X.; Lin, Y.; Lu, G. Sensitive fluorescence sensor for point-of-care detection of trypsin using glutathione-stabilized gold nanoclusters. *Sens. Actuators B Chem.* **2019**, *282*, 366–372. [CrossRef]

45. Jiang, H.; Su, X.; Zhang, Y.; Zhou, J.; Fang, D.; Wang, X. Unexpected thiols triggering photoluminescent enhancement of cytidine stabilized Au nanoclusters for sensitive assays of glutathione reductase and its inhibitors screening. *Anal. Chem.* **2016**, *88*, 4766–4771. [CrossRef] [PubMed]

46. Ni, P.; Chen, C.; Jiang, Y.; Zhang, C.; Wang, B.; Cao, B.; Li, C.; Lu, Y. Gold nanoclusters-based dual-channel assay for colorimetric and turn-on fluorescent sensing of alkaline phosphatase. *Sens. Actuators B Chem.* **2019**, *301*, 127080. [CrossRef]

47. Qu, F.; Meng, L.; Zi, Y.; You, J. Ratiometric detection of alkaline phosphatase based on aggregation-induced emission enhancement. *Anal. Bioanal. Chem.* **2019**, *411*, 7431–7440. [CrossRef]

48. You, J.G.; Tseng, W.L. Peptide-induced aggregation of glutathione-capped gold nanoclusters: A new strategy for designing aggregation-induced enhanced emission probes. *Anal. Chim. Acta* **2019**, *1078*, 101–111. [CrossRef] [PubMed]

49. Govindaraju, S.; Reddy, A.S.; Kim, J.; Yun, K. Sensitive detection of epinephrine in human serum via fluorescence enhancement of gold nanoclusters. *Appl. Surf. Sci.* **2019**, *498*, 143837. [CrossRef]

50. Ungor, D.; Horvath, K.; Dekany, I.; Csapo, E. Red-emitting gold nanoclusters for rapid fluorescence sensing of tryptophan metabolites. *Sens. Actuators B Chem.* **2019**, *288*, 728–733. [CrossRef]

51. Teng, Y.; Jia, X.; Li, J.; Wang, E. Ratiometric fluorescence detection of tyrosinase activity and dopamine using thiolate-protected gold nanoclusters. *Anal. Chem.* **2015**, *87*, 4897–4902. [CrossRef] [PubMed]

52. Zhang, X.; Wu, F.G.; Liu, P.; Gu, N.; Chen, Z. Enhanced fluorescence of gold nanoclusters composed of $HAuCl_4$ and histidine by glutathione: Glutathione detection and selective cancer cell imaging. *Small* **2014**, *10*, 5170–5177. [PubMed]

53. Liu, J.; Gan, L.L.; Yang, X.M. Glutenin-directed gold nanoclusters employed for assaying vitamin B-1. *New J. Chem.* **2020**, *44*, 487–491. [CrossRef]

54. Chen, T.; Hu, Y.; Cen, Y.; Chu, X.; Lu, Y. A Dual-Emission Fluorescent Nanocomplex of Gold-Cluster-Decorated Silica Particles for Live Cell Imaging of Highly Reactive Oxygen Species. *J. Am. Chem. Soc.* **2013**, *135*, 11595–11602. [CrossRef] [PubMed]

55. Gao, P.F.; Li, M.; Zhang, Y.; Dong, C.; Zhang, G.M.; Shi, L.H.; Li, G.; Yuan, M.J.; Shuang, S.M. Facile, rapid one-pot synthesis of multifunctional gold nanoclusters for cell imaging, hydrogen sulfide detection and pH sensing. *Talanta* **2019**, *197*, 1–11. [CrossRef]

56. Ding, C.; Tian, Y. Gold nanocluster-based fluorescence biosensor for targeted imaging in cancer cells and ratiometric determination of intracellular pH. *Biosens. Bioelectron.* **2015**, *65*, 183–190. [CrossRef]

57. Zhang, P.; Yang, X.X.; Wang, Y.; Zhao, N.W.; Xiong, Z.H.; Huang, C.Z. Rapid synthesis of highly luminescent and stable Au-20 nanoclusters for active tumor-targeted imaging in vitro and in vivo. *Nanoscale* **2014**, *6*, 2261–2269. [CrossRef]

58. Chen, H.; Li, S.; Li, B.; Ren, X.; Li, S.; Mahounga, D.M.; Cui, S.; Gu, Y.; Achilefu, S. Folate-modified gold nanoclusters as near-infrared fluorescent probes for tumor imaging and therapy. *Nanoscale* **2012**, *4*, 6050–6064. [CrossRef]

59. Pyo, K.; Ly, N.H.; Yoon, S.Y.; Shen, Y.; Choi, S.Y.; Lee, S.Y.; Joo, S.W.; Lee, D. Highly luminescent folate-functionalized Au_{22} nanoclusters for bioimaging. *Adv. Healthc. Mater.* **2017**, *6*, 1700203. [CrossRef]

60. Chen, D.; Li, B.; Cai, S.; Wang, P.; Peng, S.; Sheng, Y.; He, Y.; Gu, Y.; Chen, H. Dual targeting luminescent gold nanoclusters for tumor imaging and deep tissue therapy. *Biomaterials* **2016**, *100*, 1–16. [CrossRef]

61. Li, H.; Huang, H.; Wang, A.-J.; Feng, H.; Feng, J.-J.; Qian, Z. Simple fabrication of eptifibatide stabilized gold nanoclusters with enhanced green fluorescence as biocompatible probe for in vitro cellular imaging. *Sens. Actuators B Chem.* **2017**, *241*, 1057–1062. [CrossRef]

62. Li, H.; Chen, J.; Huang, H.; Feng, J.-J.; Wang, A.-J.; Shao, L.-X. Green and facile synthesis of l -carnosine protected fluorescent gold nanoclusters for cellular imaging. *Sens. Actuators B Chem.* **2016**, *223*, 40–44. [CrossRef]

63. Li, Z.; Peng, H.; Liu, J.; Tian, Y.; Yang, W.; Yao, J.; Shao, Z.; Chen, X. Plant Protein-Directed Synthesis of Luminescent Gold Nanocluster Hybrids for Tumor Imaging. *ACS Appl. Mater. Interfaces* **2018**, *10*, 83–90. [CrossRef] [PubMed]